

Article

Active Brownian Filamentous Polymers under Shear Flow

Aitor Martín-Gómez, Gerhard Gompper and Roland G. Winkler * 

Theoretical Soft Matter and Biophysics, Institute of Complex Systems and Institute for Advanced Simulation, Forschungszentrum Jülich, D-52425 Jülich, Germany; a.gomez@fz-juelich.de (A.M.-G.); g.gompper@fz-juelich.de (G.G.)

* Correspondence: r.winkler@fz-juelich.de

Received: 4 July 2018; Accepted: 27 July 2018; Published: 30 July 2018



Abstract: The conformational and rheological properties of active filaments/polymers exposed to shear flow are studied analytically. Using the continuous Gaussian semiflexible polymer model extended by the activity, we derive analytical expressions for the dependence of the deformation, orientation, relaxation times, and viscosity on the persistence length, shear rate, and activity. The model yields a Weissenberg-number dependent shear-induced deformation, alignment, and shear thinning behavior, similarly to the passive counterpart. Thereby, the model shows an intimate coupling between activity and shear flow. As a consequence, activity enhances the shear-induced polymer deformation for flexible polymers. For semiflexible polymers/filaments, a nonmonotonic deformation is obtained because of the activity-induced shrinkage at moderate and swelling at large activities. Independent of stiffness, activity-induced swelling facilitates and enhances alignment and shear thinning compared to a passive polymer. In the asymptotic limit of large activities, a polymer length- and stiffness-independent behavior is obtained, with universal shear-rate dependencies for the conformations, dynamics, and rheology.

Keywords: semiflexible polymer; active Brownian particle; active polymer; polymer conformations; polymer dynamics; colored noise; viscosity; rheology

1. Introduction

Active matter is composed of agents which either convert internal energy or exploit energy from the environment to generate directed motion [1–7]. The associated out-of-equilibrium character of active matter is the origin of a number of fascinating phenomena, such as activity-driven phase separation or large-scale collective motion [1–13]. On the nano- and microscale, biology provides a plethora of active agents ranging from enzymes [14,15] and the cytoskeleton in living cells [1,3,16–22] to sperm, algae, bacteria, and a diversity of other planktonic microorganisms [1,4,23,24]. Furthermore, artificial active particles have been synthesized utilizing various concepts [5,25–29]. Thereby, active agents exhibit a variety of forms and shapes—from (near) spherical (*Chlamydomonas reinhardtii*, *Volvox*) to cylindrical (*Proteus mirabilis* [30], self-assembled dinoflagellates [31,32]), and filamentous, polymer-like structures (actin filaments, microtubules, linear assemblies of Janus particles [33,34]). In fact, active systems with internal degrees of freedom, such as linear chains [7,34–54] or other forms of organization [33,34,55,56], denoted as “active colloidal molecules” in Ref. [34], are particularly interesting and give rise to novel conformational [39,41,47,52], dynamical [45,53,57–59], and collective phenomena [12,16,56,60–66]. Examples range from activity-induced polymer swelling and shrinkage [7,39,41,47,52], enhanced diffusive motion and dynamics [40,41,53,59]—as observed in microtubuli [67], actin filaments [68], chromosomal loci in simple organisms [69,70], or in the chromatin dynamics in eukaryotes [71]—to mesoscale turbulence [12,56] or streaming nematics [60,65].

In theoretical and simulation studies, filamentous, polymer-like active agents are typically described as semiflexible polymers composed of monomers, which are propelled by an active force. The properties of the active force depend on the system of interest. Actin filaments or microtubules in motility assays or motor-protein carpets [61] are driven by tangential forces with respect to the filament contour [35,43,45,66]. Alternatively, polymers comprised of active Brownian particles (ABPs) are driven by active forces, which change their propulsion direction independently in a diffusive manner [5,10,47,52,72]. So far, no polymer-like assembly of ABPs has been synthesized. However, activity can also be considered as an external random colored-noise force experienced by the polymer, as discussed in Refs. [4,6,51–53]. In this context, “activity” is an extension of the theoretical description toward more complex out-of-equilibrium environments, which break detailed balance and the fluctuation–dissipation theorem [73].

In this article, the conformational and rheological properties of an active polymer subject to colored noise and exposed to shear flow are studied. In particular, the interplay between activity and shear flow is investigated. The effect of propulsion on the rheology of entangled, isotropic solutions of tangentially driven semiflexible polymers has been addressed in Ref. [35], and an accelerated relaxation has been found at long times, resulting in a reduced low-frequency viscosity. Specifically, the transport of microorganisms and their assemblies, which is omnipresent in nature, e.g., plankton in aquatic environments and microfluidic devices, is strongly affected by fluid flow [74]. In such habitats, shear flow is pervasive and determines the destination of microorganisms. Our goal is to unravel the properties of semiflexible filamentous polymers in such an out-of-equilibrium environment induced by both colored noise and fluid flow. Our studies reveal an intimate coupling of activity and shear flow, which leads to distinct differences in the non-equilibrium polymer conformations, dynamics, and rheology. Specifically, shear-rate dependent power-laws are modified at large activities. It is noteworthy that polymer-length- and stiffness-independent universal dependencies on the shear rate are predicted in the asymptotic limit of large activities.

The article is organized as follows. Section 2 describes the model of the active polymer in shear flow and presents the equations of motion and their solution. In Section 3, results for the shear-rate dependence of the relaxation times and conformational properties are presented for various activities and stiffness. The viscosity of the polymer is considered in Section 4. Section 5 discusses the various findings, and Section 6 summarizes the major results of our study.

2. Model: Active Brownian Filament/Polymer

2.1. Equation of Motion

The filament/polymer is described by the Gaussian semiflexible polymer model [75–80]. Thereby, the polymer of length L is considered as a continuous, differentiable space curve $\mathbf{r}(s, t)$, with the contour coordinate s ($-L/2 \leq s \leq L/2$), and the time t . The activity is introduced by assigning an active velocity $\mathbf{v}(s, t)$ to every point $\mathbf{r}(s, t)$ (cf. Figure 1). The equation of motion of $\mathbf{r}(s, t)$ is then given by [52,53]

$$\frac{\partial}{\partial t} \mathbf{r}(s, t) = \mathbf{v}(s, t) + \frac{k_B T}{\gamma} \left(2\lambda \frac{\partial^2}{\partial s^2} \mathbf{r}(s, t) - \epsilon \frac{\partial^4}{\partial s^4} \mathbf{r}(s, t) \right) + \frac{1}{\gamma} \mathbf{f}(s, t) + \mathbf{K} \mathbf{r}(s, t) \quad (1)$$

with the boundary conditions

$$\left[2\lambda \frac{\partial}{\partial s} \mathbf{r}(s, t) - \epsilon \frac{\partial^3}{\partial s^3} \mathbf{r}(s, t) \right]_{s=\pm L/2} = 0, \quad \left[2\lambda_0 \frac{\partial}{\partial s} \mathbf{r}(s, t) \pm \epsilon \frac{\partial^2}{\partial s^2} \mathbf{r}(s, t) \right]_{s=\pm L/2} = 0 \quad (2)$$

The terms with the second and fourth derivative in Equation (1) account for the entropy elasticity and bending stiffness, respectively, \mathbf{f} for thermal fluctuations, and $\mathbf{K} \mathbf{r}(s, t)$ for the shear flow, with the shear-rate tensor \mathbf{K} . The Lagrangian multipliers $\lambda_0 = \lambda(\pm L/2)$, $\lambda(s)$, and ϵ are determined by

constraints [81,82]. In general, this yields $\epsilon = 3/4p$ and $\lambda_0 = 3/4$ for a polymer in three dimensions, where $p = 1/2l_p$ in terms of the persistence length l_p [75,82]. The Lagrangian multiplier λ , denoted as stretching coefficient, is determined in a mean-field manner via the global constraint [52,75,82]:

$$\int_{-L/2}^{L/2} \left\langle \left(\frac{\partial \mathbf{r}(s,t)}{\partial s} \right)^2 \right\rangle ds = L \quad (3)$$

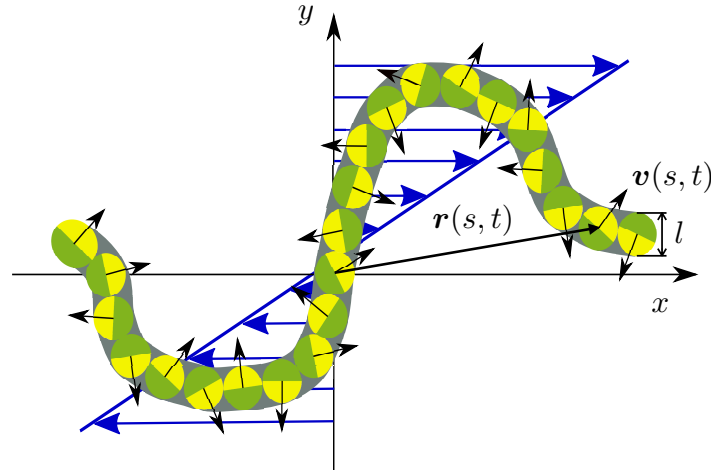


Figure 1. Illustration of the continuous semiflexible active polymer (ABPO) in shear flow. The arrows and colors indicate the orientation of the active velocity $\mathbf{v}(s,t)$.

As discussed in Ref. [52], the active velocity $\mathbf{v}(s,t)$ can be considered as external colored noise experienced by the respective polymer site, the picture adopted here, or as intrinsic polymer property originating from self-propulsion. For an identical mathematical formulation, the active site has then to be described by an active Ornstein–Uhlenbeck particle (AOUP) [73,83]. However, also an active Brownian particle (ABP) can be considered, as long as only second moments of the active velocity correlation function are relevant [57]. In any case, the active velocity is described by a diffusive process—Brownian motion—either for the propulsion direction only (ABPs) [4–6,10,84,85], or for the individual Cartesian components, i.e., the magnitude of \mathbf{v} is changing too (AOUPs) [4,52,73,83]. Independent of the details of the underlying stochastic (active) processes, we denote our polymer as active Brownian polymer (ABPO). Hence, the active velocity, $\mathbf{v}(s,t)$, is described by a non-Markovian, but Gaussian stochastic process with zero mean and the second moments [52,53,73]

$$\langle v_\alpha(s,t) v_\beta(s',t') \rangle = \frac{v_0^2 l}{3} e^{-\gamma_R |t-t'|} \delta(s-s') \delta_{\alpha\beta} \quad (4)$$

i.e., the polymer is exposed to colored noise [52,53,73]. Here, v_0 is the propulsion velocity, the damping factor γ_R can be related to the rotational diffusion coefficient D_R of a spherical colloid in three dimensions via $\gamma_R = 2D_R$, and $\alpha, \beta \in \{x, y, z\}$. We introduce the length scale l in the continuum representation of a semiflexible polymer. Thereby, the ratio L/l can be interpreted as the number of uniformly distributed active sites along the polymer. In the flexible limit, we set $p = 1/l$, which leads to the relation $pL = L/l$. The effect of the ratio L/l on the conformational properties in the absence of shear has briefly been addressed in Ref. [52]. The choice $p = 1/l$ is motivated by discrete bead-spring polymers, typically used in computer simulations [57,86], where every monomer is an ABP. The stochastic process $\mathbf{\Gamma}(s,t)$ of the translational motion is assumed to be stationary, Markovian, and Gaussian with zero mean and the second moments

$$\langle \mathbf{\Gamma}_\alpha(s,t) \mathbf{\Gamma}_\beta(s',t') \rangle = 2\gamma k_B T \delta_{\alpha\beta} \delta(s-s') \delta(t-t') \quad (5)$$

where T is the temperature, k_B the Boltzmann constant, and γ the translational friction coefficient per length. The latter is related with the translational, thermal diffusion coefficient D_T via $D_T = k_B T / \gamma l$. Finally, shear is applied along the x -direction and the gradient along the y -direction of the Cartesian reference frame. Hence, the shear-rate tensor is given by $K_{xy} = \dot{\gamma}$, where $\dot{\gamma}$ is the shear rate.

2.2. Eigenfunction Expansion

The linear equation of motion (1) is solved by the eigenfunction expansion

$$\mathbf{r}(s, t) = \sum_{n=0}^{\infty} \chi_n(t) \varphi_n(s) \quad (6)$$

and an analogous representation of \mathbf{v} and \mathbf{I} , in terms of the eigenfunctions φ_n of the eigenvalue equation [52,76]

$$\epsilon k_B T \frac{\partial^4}{\partial s^4} \varphi_n(s) - 2\lambda k_B T \frac{\partial^2}{\partial s^2} \varphi_n(s) = \zeta_n \varphi_n(s) \quad (7)$$

The respective eigenfunctions are

$$\varphi_0 = \sqrt{\frac{1}{L}} \quad (8)$$

$$\varphi_n(s) = \sqrt{\frac{c_n}{L}} \left(\zeta'_n \frac{\sinh(\zeta'_n s)}{\cosh(\zeta'_n L/2)} + \zeta_n \frac{\sin(\zeta_n s)}{\cos(\zeta_n L/2)} \right), \quad \forall n \text{ odd} \quad (9)$$

$$\varphi_n(s) = \sqrt{\frac{c_n}{L}} \left(\zeta'_n \frac{\cosh(\zeta'_n s)}{\sinh(\zeta'_n L/2)} - \zeta_n \frac{\cos(\zeta_n s)}{\sin(\zeta_n L/2)} \right), \quad \forall n \text{ even} \quad (10)$$

with the relations between the wave numbers ζ_n , ζ'_n , and the eigenvalues ζ_n ($n \in \mathbb{N}$)

$$\zeta_n'^2 - \zeta_n^2 = \frac{2\lambda}{\epsilon}, \quad \zeta_0 = 0, \quad \zeta_n = k_B T (\epsilon \zeta_n^4 + 2\lambda \zeta_n^2) \quad (11)$$

The eigenfunction φ_0 accounts for the polymer's center of mass motion. The c_n s are normalization coefficients, and the wave numbers are determined by the boundary conditions (2).

Insertion of Equation (6) into Equation (1) yields the equation of motion for the mode amplitudes χ_n ,

$$\frac{\partial}{\partial t} \chi_{n\alpha}(t) = -\frac{1}{\tau_n} \chi_{n\alpha}(t) + v_{n\alpha}(t) + \frac{1}{\gamma} \mathbf{I}_{n\alpha}(t) + \dot{\gamma} \chi_{ny} \delta_{x\alpha} \quad (12)$$

with respective amplitudes $v_n(t)$ and $\mathbf{I}_n(t)$ of the active velocity and stochastic force, and the relaxation times ($n > 0$)

$$\tau_n = \frac{\gamma}{\zeta_n} = \frac{\gamma}{k_B T (\epsilon \zeta_n^4 + 2\lambda \zeta_n^2)} \quad (13)$$

The stationary-state solution of Equation (12) for $n > 0$ is

$$\chi_{n\alpha}(t) = \int_{-\infty}^t dt' e^{-(t-t')/\tau_n} [v_{n\alpha}(t') + \mathbf{I}_{n\alpha}(t') + \dot{\gamma} \chi_{ny}(t') \delta_{x\alpha}] \quad (14)$$

and for $n = 0$

$$\chi_{0\alpha}(t) = \chi_{0\alpha}(0) + \int_0^t dt' [v_{0\alpha}(t') + \mathbf{I}_{0\alpha}(t') + \dot{\gamma} \chi_{0y}(t') \delta_{x\alpha}] \quad (15)$$

2.3. Mode–Amplitude Correlation Functions

The time correlation functions of the mode amplitudes can be calculated straightforwardly by Equation (14), which yields $\langle \chi_n(t) \cdot \chi_m(t') \rangle = \delta_{nm} \langle \chi_n(t) \cdot \chi_n(t') \rangle$, with $(n > 0, t \geq 0)$

$$\langle \chi_{ny}(t) \chi_{ny}(0) \rangle = \langle \chi_{nz}(t) \chi_{nz}(0) \rangle = \left(\frac{k_B T \tau_n}{\gamma} - \frac{v_0^2 l \gamma_R \tau_n^3}{3(1 - (\gamma_R \tau_n)^2)} \right) e^{-t/\tau_n} + \frac{v_0^2 l \tau_n^2}{3(1 - (\gamma_R \tau_n)^2)} e^{-\gamma_R t} \quad (16)$$

$$\begin{aligned} \langle \chi_{nx}(t) \chi_{nx}(0) \rangle &= \langle \chi_{ny}(t) \chi_{ny}(0) \rangle + \frac{\gamma^2 v_0^2 l \tau_n^4}{3(1 - (\gamma_R \tau_n)^2)^2} e^{-\gamma_R t} \\ &+ \left[\frac{\gamma^2 \tau_n^2}{2} \left(\frac{k_B T \tau_n}{\gamma} - \frac{v_0^2 l \gamma_R \tau_n^3}{3(1 - (\gamma_R \tau_n)^2)} \right) \left(1 + \frac{t}{\tau_n} \right) - \frac{\gamma^2 \gamma_R v_0^2 l \tau_n^5}{3(1 - (\gamma_R \tau_n)^2)^2} \right] e^{-t/\tau_n} \end{aligned} \quad (17)$$

$$\begin{aligned} \langle \chi_{nx}(t) \chi_{ny}(0) \rangle &= \frac{\gamma v_0^2 l \tau_n^3}{3(1 - (\gamma_R \tau_n)^2)(1 - \gamma_R \tau_n)} e^{-\gamma_R t} \\ &+ \left[\frac{\gamma \tau_n}{2} \left(\frac{k_B T \tau_n}{\gamma} - \frac{v_0^2 l \gamma_R \tau_n^3}{3(1 - (\gamma_R \tau_n)^2)} \right) \left(1 + \frac{2t}{\tau_n} \right) - \frac{2\gamma \gamma_R v_0^2 l \tau_n^4}{3(1 - (\gamma_R \tau_n)^2)^2} \right] e^{-t/\tau_n} \end{aligned} \quad (18)$$

2.4. Inextensibility and Stretching Coefficient λ

The inextensibility constraint (3), together with the eigenfunction expansion and the correlation functions (16)–(18), leads to the equation

$$\sum_{n=1}^{\infty} \langle \chi_n^2 \rangle \phi_n = 1 \quad (19)$$

to determine λ , where $\phi_n = \int_{-L/2}^{L/2} (\partial \phi_n(s) / \partial s)^2 ds / L$ and

$$\langle \chi_n^2 \rangle = \frac{3k_B T}{\gamma} \tau_n + \frac{v_0^2 l}{1 + \gamma_R \tau_n} \tau_n^2 + \gamma^2 \frac{k_B T}{2\gamma} \tau_n^3 + \gamma^2 \frac{v_0^2 l (2 + \gamma_R \tau_n)}{6(1 + \gamma_R \tau_n)^2} \tau_n^4 \quad (20)$$

In general, Equation (19) has to be solved numerically. However, the sum over the mode numbers can be evaluated in the limit $pL \rightarrow \infty$, or even for moderate pL , for larger activities $Pe \gg 1$ [53], due to the dominance of the stretching modes in these limits, i.e., $\zeta_n = n\pi/L$ and $\tau_n = \gamma L^2 / 3k_B T \pi^2 p \mu n^2 = \tau_R / \mu n^2$, where $\tau_R = \gamma L^2 / 3k_B T \pi^2 p$ is the Rouse relaxation time of the passive polymer [76,87]. Here, the Péclet number Pe and other relevant dimensionless quantities, such as the Weissenberg number Wi , the ratio between the translational and rotational diffusion coefficient Δ , and the scaled stretching coefficient μ , in terms of the value at equilibrium, $3p/2$, are introduced as

$$Pe = \frac{v_0}{D_R l}, \quad Wi = \gamma \tau_0, \quad \Delta = \frac{D_T}{l^2 D_R}, \quad \mu = \frac{2\lambda}{3p} \quad (21)$$

Thereby, $\tau_0 = \tau_1(Pe, Wi = 0)$ is the longest polymer relaxation time at zero shear but in the presence of activity. Combined with results from Refs. [52,88], we find from Equation (19)

$$\begin{aligned} \frac{1}{\sqrt{\mu}} \coth(2pL\sqrt{\mu}) - \frac{1}{2pL\mu} + \frac{Pe^2}{6\mu\Delta} \left[\sqrt{\frac{\mu}{1 + 6\mu^2 p^3 l^3 \Delta}} \coth\left(2pL\sqrt{\frac{\mu}{1 + 6\mu^2 p^3 l^3 \Delta}}\right) - \frac{1}{2pL} \right] \\ + \frac{Wi^2 \pi^4}{540pL} \frac{\mu_0^2}{\mu^3} + \frac{Wi^2 Pe^2 L^3 (2 + 2L^3 / 3\pi^2 l^3 \Delta p L \mu)}{54\pi^2 \Delta^2 (pL)^2 l^3 (1 + 2L^3 / 3\pi^2 l^3 \Delta p L \mu)^2} \frac{\mu_0^2}{\mu^4} = 1 \end{aligned} \quad (22)$$

where for the evaluation of the term proportional to $Wi^2Pe^2 \sim \dot{\gamma}^2 v_0^2$ only the first mode, $n = 1$, has been taken into account; the deviation to the full sum is below 3% for all Pe, pL , and Wi . The last term on the left-hand side reflects the coupling between activity and shear flow.

The following asymptotic dependencies for the stretching coefficient μ are obtained:

- (i) Passive semiflexible polymer in shear flow, i.e., $Pe = 0$ (for details, cf. Ref. [88])

- For $pL \gg 1$ and $\mu \gg 1$

$$\mu^3 - \mu^{5/2} - \frac{\pi^4 Wi^2}{540 pL} = 0, \quad \xrightarrow{Wi \gg 1} \mu = Wi^{2/3} \left(\frac{\pi^4}{540 pL} \right)^{1/3} \quad (23)$$

- For $pL < 1$ and $\mu \gg 1$

$$\mu = \frac{Wi^{2/3}}{pL} \left(\frac{4}{15} \right)^{1/3} \quad (24)$$

- (ii) Active flexible polymer at weak shear flow, i.e., $Wi \ll 1$, $pL \gg 1$, and $\tau_n = \tau_R / \mu_0 n^2$ [52,53]. For later use, we denote the Lagrangian multiplier at $Wi = 0$ and $Pe > 0$ by μ_0

- For $1 \ll Pe < \infty$ and $\mu_0 \rightarrow \infty$

$$\mu_0 = \frac{Pe^{4/3}}{pL} \frac{L}{6l\Delta} \quad (25)$$

- For $Pe \rightarrow \infty$, i.e., $\mu_0 \rightarrow \infty$

$$\mu_0 = \frac{Pe}{pL\Delta} \sqrt{\frac{L^3}{54l^3}} \quad (26)$$

- (iii) Active flexible polymer in shear flow, $\tau_n = \tau_R / \mu n^2$,

- For $1 < Pe, Wi < \infty$, $L^3 / 3\pi l^3 pL\Delta\mu \gg 1$, and $pL \gg 1$ (with Equation (25))

$$\mu = Wi^{2/3} \mu_0^{2/3} \left(\frac{Pe^2}{36\Delta pL} \right)^{1/3} = Wi^{2/3} \frac{Pe^{14/9}}{pL\Delta} \left(\frac{L}{36l} \right)^{2/3} \quad (27)$$

- For $Pe \rightarrow \infty$, i.e., $\mu_0 = Pe\sqrt{L^3/54l^3}/pL\Delta \rightarrow \infty$

$$\mu = \mu_0 \frac{1}{\sqrt{2}} \sqrt{1 + \sqrt{1 + \frac{8Wi^2}{\pi^2}}} \xrightarrow{Wi \gg 1} Wi^{1/2} \frac{Pe}{pL\Delta} \sqrt{\frac{\sqrt{2}L^3}{54\pi l^3}} \quad (28)$$

Hence, in the limit $Wi \rightarrow \infty$, μ exhibits a crossover from a $\mu \sim Wi^{2/3}$ dependence for $1 \ll Pe < \infty$ to a dependence $\mu \sim Wi^{1/2}$ for $Pe \rightarrow \infty$. The latter characteristics are different from the passive case and are a consequence of the coupling between activity and shear flow.

The full numerical solution for the stretching coefficient μ is presented in Figure 2 as a function of the Weissenberg number and for various activities. We set $L/l = 10^2$ for the number of active sites. Hence, when changing pL , we change the persistence length $l_p = 1/2p$ at a fixed contour length in order to maintain the active-site density. As illustrated for $pL = 0.1$ and $pL = 10^2$, μ exhibits a crossover from a dependence $\mu \sim Wi^{2/3}$ at low Pe to the relation $\mu \sim Wi^{1/2}$ for $Pe \rightarrow \infty$ and sufficiently large Wi , in agreement with the theoretical limits, Equations (27) and (28). We like to emphasize that μ/μ_0 approaches the asymptotic dependence

$$\frac{\mu}{\mu_0} = \sqrt{Wi} \sqrt{\frac{\sqrt{2}}{\pi}} \quad (29)$$

for $Pe \gg 1$. Hence, a universal, activity- and pL -independent behavior is predicted. For completeness, Figure 3 illustrates the dependence of μ on the Péclet number for the Weissenberg numbers $Wi = 0$ (left) and $Wi = 10^2$ (right). The predicted power-law dependencies (Equation (25) for $Wi < 1$, and Equation (28) for $Pe \gg 1$ and $Wi \ll Pe$) and scaling with respect to pL are recovered. Figure 2 shows a shift of the crossover from the $Wi^{2/3}$ to the $Wi^{1/2}$ dependence towards smaller Wi with increasing Pe . This crossover strongly depends on L/l , and shifts to larger Wi with increasing L/l . Hence, for a larger number of active sites, no crossover could be observed anymore for suitable Weissenberg numbers. On the contrary, for a smaller number L/l , the crossover appears already at smaller Wi . In the extreme case of $L/l \rightarrow 1$, a behavior similar to an active dumbbell in shear flow appears [51].

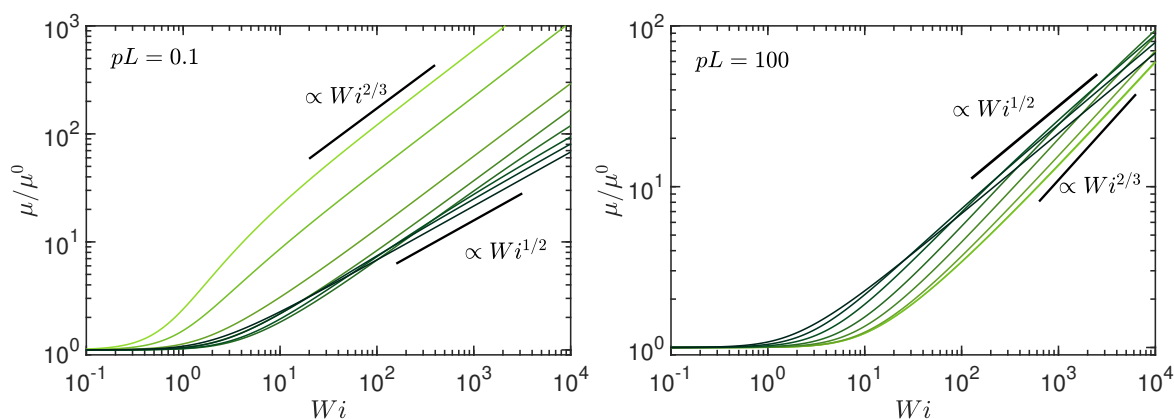


Figure 2. Stretching coefficient $\mu = 2\lambda/3p$ normalized by the value μ_0 of the active, non-sheared system as function of the Weissenberg number Wi for the Péclet numbers $Pe = 0, 0.6, 3, 10, 30, 10^2, 3 \times 10^2$, and ∞ (bright to dark color); (left) $pL = L/2l_p = 0.1$ (stiff) and (right) $pL = 10^2$ (flexible polymer). The number of active sites is $L/l = 10^2$ and the diffusion coefficient ratio $\Delta = 0.3$.

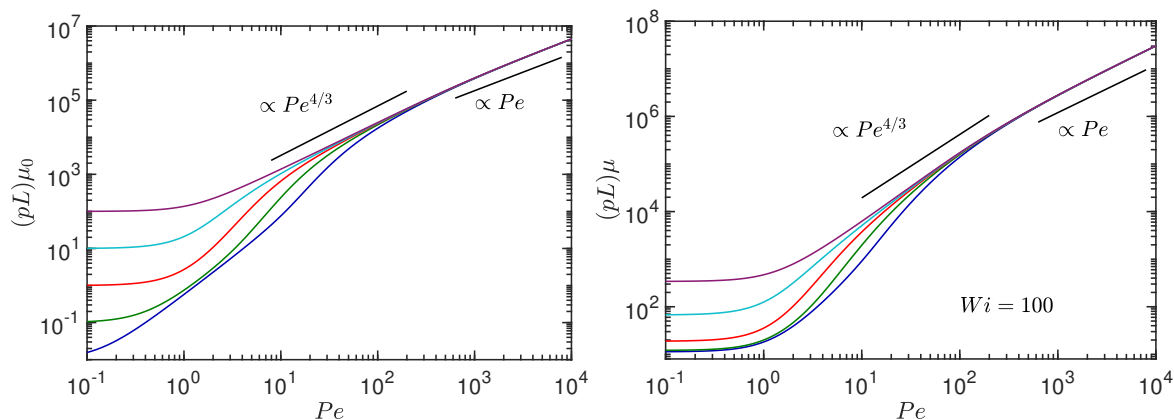


Figure 3. Stretching coefficient $\mu = 2\lambda/3p$ as a function of the Péclet number Pe for the stiffness $pL = 10^{-2}, 10^{-1}, 10^0, 10^1$, and 10^2 (bottom to top). The Weissenberg numbers are (left) $Wi = 0$ [52] and (right) $Wi = 10^2$. The number of active sites is $L/l = 10^2$ and $\Delta = 0.3$.

3. Dynamics and Conformations

3.1. Relaxation Times

The relaxation times (13) depend on the shear rate (Wi), activity (Pe), and persistence length (p) via the stretching coefficient $\lambda = 2\mu/3p$. In the limit of a highly flexible polymer, the relaxation time is $\tau_n = \tau_R/(\mu n^2)$. Hence, the mode-number dependence of τ_n is unaffected by the nonequilibrium character of the dynamics. However, the presence of μ indicates the fundamental importance to account for the inextensibility of the polymer. Since $\mu \geq 1$ is a monotonically increasing function of Pe and Wi , activity and shear flow always accelerate the relaxation process and the relaxation times become shorter [35,53].

Figure 4 displays the numerically obtained longest relaxation time as a function of the Weissenberg number for various Pe and the stiffness $pL = 0.1$ (stiff) and $pL = 10^2$ (flexible polymer). For $pL \ll 1$ and small Péclet numbers ($Pe \lesssim 1$), the relaxation time τ_1 , corresponding to the rotation relaxation time of a rigid polymer, dominates over all other (bending) relaxation times [53,76]. Hence, the relaxation times of Figure 4 (left) are not simply proportional to μ^{-1} in this limit. However, with increasing Pe , bending contributions gradually vanish and the asymptotic dependence $\tau_1/\tau_0 = \mu_0/\mu$ is assumed. According to Equation (29), the ratio τ_1/τ_0 is then independent of Pe and pL . In Figure 4 (right) for flexible polymers, bending modes are negligibly small and the relation $\tau_1 \sim 1/\mu$ applies for all Pe . Consequently, τ_1 exhibits the power-law dependencies of Equations (23), (27), and (28).

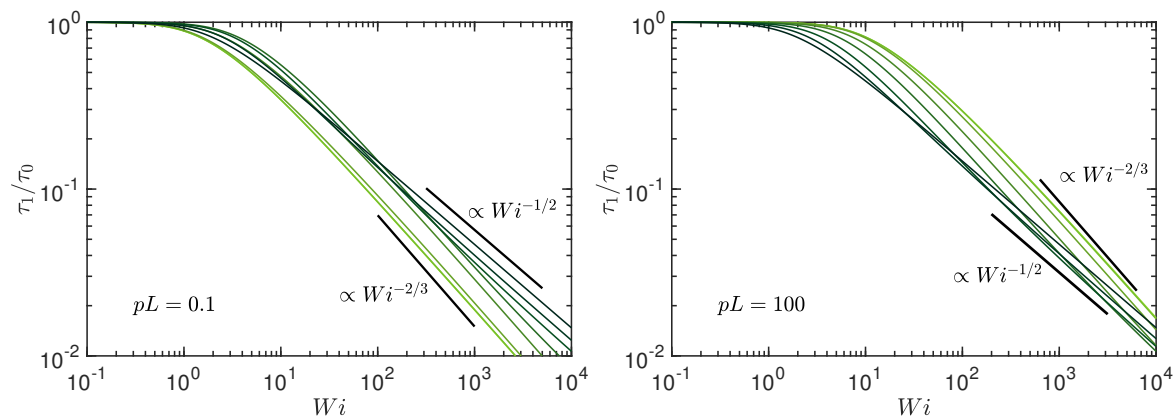


Figure 4. Longest polymer relaxation time τ_1 normalized by the longest relaxation time τ_0 of the active, non-sheared system ($Wi = 0$) as function of the Weissenberg number Wi for the Péclet numbers $Pe = 0, 0.6, 3, 10, 30, 10^2, 3 \times 10^2$, and ∞ (bright to dark color); **(left)** $pL = 0.1$ and **(right)** $pL = 10^2$. The number of active sites is $L/l = 10^2$ and $\Delta = 0.3$.

We like to emphasize that the shear-rate dependency $\tau_1 \sim 1/\sqrt{Wi}$ is a consequence of the activity of the polymer and emerges from the coupling of activity and shear (cf. Equation (22)). The passive polymer under shear exhibits the dependence $\tau_1 \sim Wi^{-2/3}$, which we find for small Pe also for the active polymer. A dumbbell of active monomers exhibits a similar coupling of activity and shear and, correspondingly, shows a comparable crossover of the relaxation times [88].

Figure 5 illustrates the mode-number dependence of the relaxation times for various activities and shear rates. For semiflexible polymers, activity and shear flow modify the relaxation behavior because stretching modes (n^2) dominate over bending modes (n^4) with increasing activity and flow strength. Bending stiffness remains dominant at larger mode numbers. Activity as well as flow induce a transition from semiflexible to flexible polymer behavior, which extends to smaller and smaller length scales with increasing Pe and Wi .

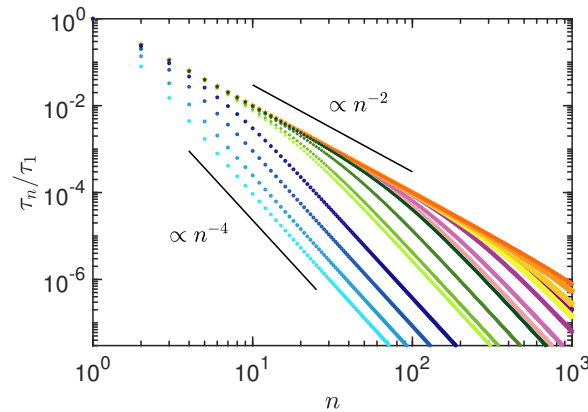


Figure 5. Mode-number dependence of the relaxation times τ_n normalized by the longest relaxation time τ_1 for the Péclet numbers $Pe = 0, 10^1, 10^2$, and 10^3 (different colors and symbols; from left to right), and the Weissenberg numbers $Wi = 0, 10^1, 10^2$, and 10^3 (different tone, bright to dark, for every color). The persistence length is $pL = 1$ and $L/l = 10^2$.

3.2. Radius of Gyration

The polymer conformations are characterized by the radius of gyration tensor G , with the components

$$G_{\alpha\beta} = \frac{1}{L} \int_{-L/2}^{L/2} \langle (r_\alpha(s) - r_{cm\alpha}) (r_\beta(s) - r_{cm\beta}) \rangle ds \quad (30)$$

where r_{cm} is the center-of-mass position of the polymer. Insertion of the eigenfunction expansion (6) yields

$$G_{\alpha\beta} = \frac{1}{L} \sum_{n=1}^{\infty} \langle \chi_{n\alpha}(t) \chi_{n\beta}(t) \rangle \quad (31)$$

in terms of the mode-amplitude correlation functions $\langle \chi_{n\alpha} \chi_{n\beta} \rangle$ (Equations (16)–(18)).

Figure 6 depicts the radius of gyration-tensor component G_{xx} along the flow direction for rather stiff ($pL = 0.1$) and highly flexible ($pL = 10^2$) polymers. Note that only the excess deformation due to shear is shown. Activity leads to additional conformational changes, which are included in $G_{xx}^0 = G_{xx}(Wi = 0)$. As for passive semiflexible polymers, shear leads to an extension and alignment along the flow direction, which saturates at large shear rates because of the finite polymer contour length [88,89]. The actual asymptotic stretching for $Wi \rightarrow \infty$ depends on the activity. At $pL \gg 1$, the asymptotic limits are $G_{xx}^\infty/G_{xx}^0 = 12pL/7$ for $Pe = 0$ [88], and $G_{xx}^\infty = L^2\pi^6/9450$, $G_{xx}^0 = L^2/45$, hence $G_{xx}^\infty/G_{xx}^0 = \pi^6/210$ for $Pe \rightarrow \infty$. It is noteworthy that the latter limit is independent of pL , i.e., it applies for every stiffness, and the same asymptotic behavior is displayed in Figure 6 (left) and (right). Shear flow leads to an additional stretching of the active polymer, particularly for $Pe \rightarrow \infty$, and not simply to an orientational alignment as for a rod, where $G_{xx}^\infty/G_{xx}^0 = 3$ for $Wi \gg 1$ [88], since $\pi^6/210 \approx 4.6 > 3$. However, the difference of the asymptotic values for $Pe = 0$ and $Pe \rightarrow \infty$, respectively, can be substantial, since G_{xx}^∞ of the passive system depends on polymer length. The polymer pre-stretching by activity reduces the possible stretching by shear. The asymptotic limits for $pL \rightarrow 0$ at $Pe = 0$ are $G_{xx}^\infty = 10L^2/105$ and $G_{xx}^0 = L^2/36$, hence, $G_{xx}^\infty/G_{xx}^0 = 24/7$, in agreement with Figure 6 (left). Note that G_{xx}/G_{xx}^0 depends non-monotonically on the Péclet number at small pL . The ratio G_{xx}/G_{xx}^0 increases with increasing Pe at small Pe and decreases again for $Pe \gg 1$ (cf. Figure 6 (left)). In contrast, G_{xx}/G_{xx}^0 decrease monotonically with increasing Pe at large pL (cf. Figure 6 (right)). In any case, shear leads to an alignment and additional stretching even in the limit of very large activity.

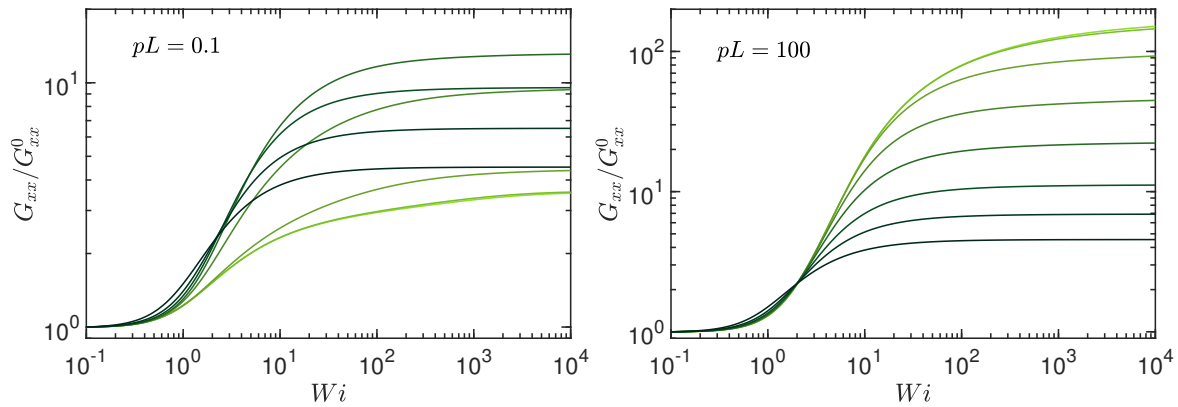


Figure 6. Radius of gyration-tensor component G_{xx} along the flow direction normalized by the value G_{xx}^0 at zero shear as function of the Weissenberg number Wi for the Péclet numbers $Pe = 0, 0.6, 3, 10, 30, 10^2, 3 \times 10^2$, and ∞ (bright to dark color); (left) $pL = 0.1$ and (right) $pL = 10^2$. The number of active sites is $L/l = 10^2$ and $\Delta = 0.3$.

The radius of gyration-tensor component along the gradient direction is displayed in Figure 7. Note that $G_{yy} \equiv G_{zz}$. Consistent with the extension in the flow direction, a polymer shrinks in the transverse direction. We find the asymptotic dependencies for $Wi \rightarrow \infty$ and $Pe = 0$, $G_{yy}/G_{yy}^0 = \sqrt[3]{30}Wi^{-2/3}$ for $pL \rightarrow 0$, and $G_{yy}/G_{yy}^0 = \sqrt[3]{540pL/\pi^4}Wi^{-2/3}$ for $pL \gg 1$. In the limit $Pe \rightarrow \infty$, $G_{yy}/G_{yy}^0 = \pi/(\sqrt{2}Wi)$ independent of pL . Again, the latter dependence is specific for active systems, since passive polymers typically show a weaker dependence on the Weissenberg number [88,89].

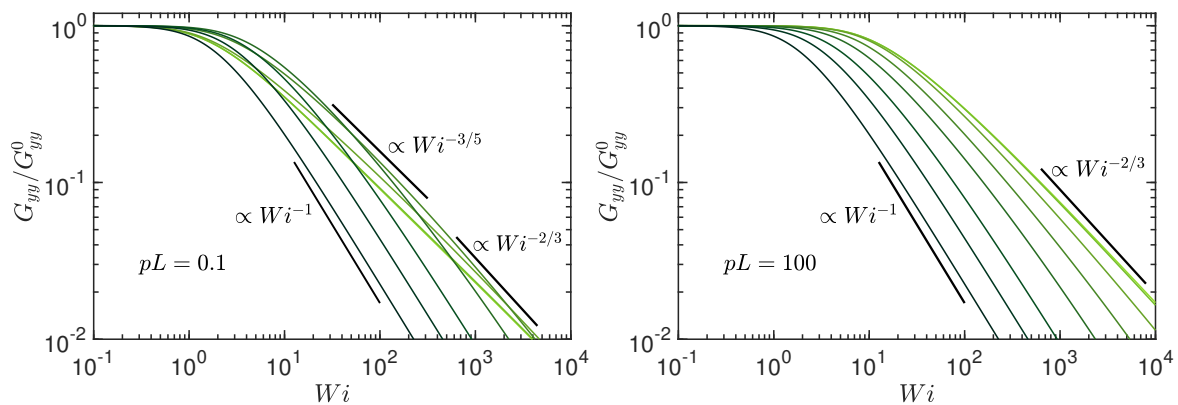


Figure 7. Radius of gyration-tensor component G_{yy} along the gradient direction normalized by the value G_{yy}^0 at zero shear as function of the Weissenberg number Wi for the Péclet numbers $Pe = 0, 0.6, 3, 10, 30, 10^2, 3 \times 10^2$, and ∞ (bright to dark color); (left) $pL = 0.1$ and (right) $pL = 10^2$. The number of active sites is $L/l = 10^2$ and $\Delta = 0.3$.

3.3. Alignment

Anisotropic objects in shear flow are preferentially aligned along the flow direction [88,89]. We characterize the extent of alignment by the angle χ_G between the eigenvector of the gyration tensor with the largest eigenvalue and the flow direction. The alignment angle is conveniently obtained from the relation

$$\tan(2\chi_G) = \frac{2G_{xy}}{G_{xx} - G_{yy}} = \frac{\sum_{n=1}^{\infty} \langle \chi_{nx} \chi_{ny} \rangle}{\sum_{n=1}^{\infty} \langle \chi_{nx}^2 \rangle - \langle \chi_{ny}^2 \rangle} \quad (32)$$

where

$$\langle \chi_{nx} \chi_{ny} \rangle = \frac{\dot{\gamma} k_B T}{2\gamma} \tau_n^2 + \frac{\dot{\gamma} v_0^2 l (2 + \gamma_R \tau_n)}{6(1 + \gamma_R \tau_n)^2} \tau_n^3 \quad (33)$$

In the asymptotic limit $\mu \gg 1$, i.e., $\tau_n \approx \tau_R / n^2 \mu$, this expression reduces to [51]

$$\tan(2\chi_G) = \frac{2\mu}{Wi\mu_0} \quad (34)$$

Hence, we obtain the asymptotic dependence $\tan(2\chi_G) \sim Wi^{-1/3}$ for $Pe \rightarrow 0$ and $\tan(2\chi_G) \sim Wi^{-1/2}$ for $Pe \rightarrow \infty$, respectively. The various regimes are displayed in Figure 8. For $Wi < 1$, the stretching coefficient is approximately unity and $\tan(2\chi_G)$ decreases as Wi^{-1} . For large Weissenberg numbers, the shear-rate dependence of μ becomes important and changes the Wi dependence to $\tan(2\chi) \sim Wi^{-1/3}$ for $Pe \ll 1$ and to $\tan(2\chi) \sim Wi^{-1/2}$ for $Pe \gg 1$.

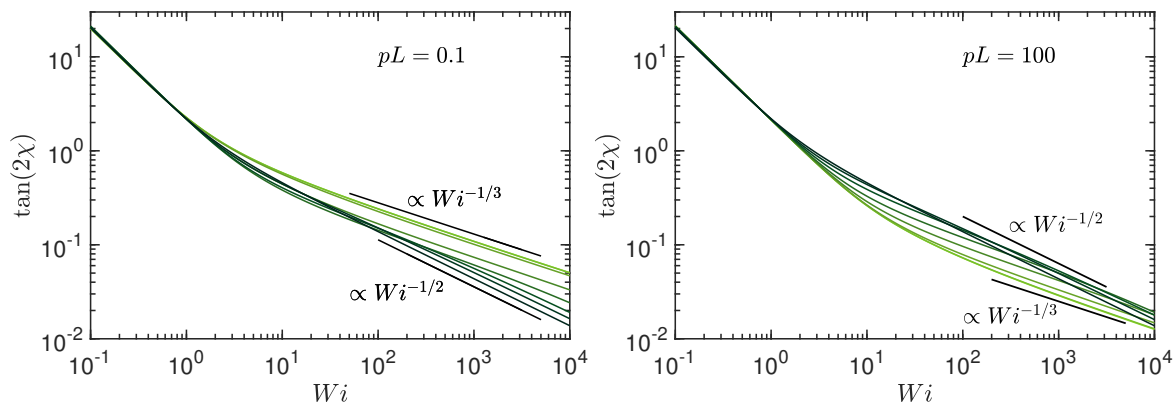


Figure 8. Shear-induced polymer alignment, characterized by the angle χ_G between the eigenvector of the gyration tensor with the largest eigenvalue and the flow direction, as function of the Weissenberg number Wi . The Péclet numbers are $Pe = 0, 0.6, 3, 10, 30, 10^2, 3 \times 10^2$, and ∞ (bright to dark color); (left) $pL = 0.1$ and (right) $pL = 10^2$. The number of active sites is $L/l = 10^2$ and $\Delta = 0.3$.

4. Rheology: Viscosity

The polymer contribution η_p to the viscosity of a dilute solution follows from the virial expression of the stress tensor

$$\sigma_{xy} = -\rho \int_{-L/2}^{L/2} \langle F_x(s) r_y(s) \rangle ds \quad (35)$$

via $\eta_p = \sigma_{xy} / \dot{\gamma}$, where F is the intramolecular force of Equation (1) and ρ the polymer concentration. The active force, $\gamma v(s, t)$, does not contribute to the stress tensor. Evaluation of the average in Equation (35) yields

$$\eta_p = \frac{\rho k_B T \gamma}{\dot{\gamma}} \sum_{n=1}^{\infty} \frac{1}{\tau_n} \langle \chi_{nx} \chi_{ny} \rangle = \frac{\rho k_B T}{2} \sum_{n=1}^{\infty} \left[\tau_n + \frac{\gamma v_0^2 l (2 + \gamma_R \tau_n)}{3k_B T (1 + \gamma_R \tau_n)^2} \tau_n^2 \right] \quad (36)$$

which depends via the stretching coefficient μ on the shear rate.

The zero-shear viscosity η_p^0 follows from Equation (36) via the stretching coefficient μ_0 . Its dependence on Pe is shown in Figure 9. The viscosity η_p^{00} at zero shear and zero Péclet number is given by $\eta_p^{00} = \rho k_B T \pi^2 \tau_R / 12$ for $pL \gg 1$, and by $\eta_p^{00} = \gamma L^3 \rho / 72$ for $Pe \rightarrow 0$. In the latter case, the first mode, $\tau_1 = \gamma L^3 / 36 k_B T$, describing the rotational motion of the rodlike polymer, dominates the sum over the relaxation times [76]. For flexible polymers, where $pL \gg 1$, the zero-shear viscosity

increases monotonically with increasing Pe , and saturates at $\eta_p^0/\eta_p^{00} = 4pL/5$ in the limit $Pe \rightarrow \infty$. Thereby, the viscosity increase, associated with the monotonic swelling of the polymer with increasing activity [52], is substantial because $\eta_p^0/\eta_p^{00} \sim pL$. With increasing stiffness, the activity-induced polymer shrinkage (cf. Ref. [52]) implies a decrease in η_p^0 , followed by an increase due to a reswelling of the polymer for $Pe \rightarrow \infty$, and the asymptotic value $\eta_p^0/\eta_p^{00} = 8/5$ is assumed. Here, the activity dependence of η_p^0 is significantly smaller than for flexible polymers, and reduces to a factor below two in the rod limit.

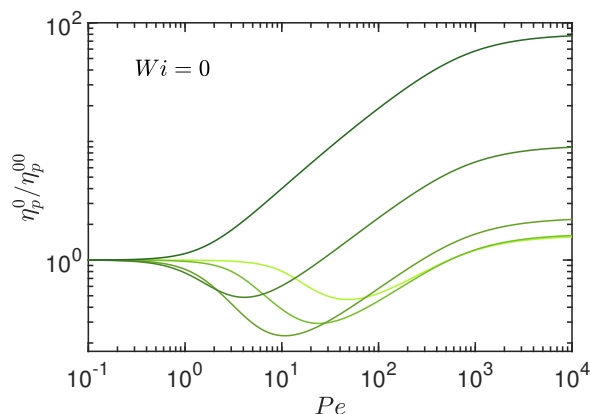


Figure 9. Zero-shear viscosity η_p^0 normalized by the zero-shear viscosity η_p^{00} of a passive polymer as function of the Péclet number Pe for the polymer stiffness $pL = 100, 10, 1, 0.1$, and 0.01 (top to bottom at $Pe = 10^4$, dark to bright color). The number of active sites is $L/l = 10^2$ and $\Delta = 0.3$.

The shear-rate dependence of the viscosity η_p , normalized by η_p^0 , is displayed in Figure 10 for various Péclet numbers. Independent of persistence length and activity, the polymers exhibit shear thinning. However, the dependence on the Weissenberg number is strongly affected by the activity. The behavior of passive semiflexible polymers, where $Pe = 0$, has been discussed theoretically in Ref. [88]. For such polymers, the viscosity exhibits the asymptotic dependencies for $Wi \rightarrow \infty$: $\eta_p/\eta_p^0 = (540pL/\pi^4)^{1/3}Wi^{-2/3}$ for $pL \gg 1$ and $\eta_p/\eta_p^0 = (30)^{1/3}Wi^{-2/3}$ for $pL < 1$. In fact, for large stiffness, $pL = L/2l_p < 1$, there is a cross-over regime with an approximate power-law drop of $\eta_p \sim Wi^{-3/5}$ as indicated in Figure 10 (left). Here, both bending and stretching modes contribute with a Weissenberg number-dependent weight. Activity substantially changes the shear-thinning behavior, and, with increasing Pe , the ratio η_p/η_p^0 decreases faster with increasing shear rate. From Equation (36), we obtain the relation

$$\frac{\eta_p}{\eta_p^0} = \frac{\mu_0^2}{\mu^2} \stackrel{Wi \rightarrow \infty}{=} \frac{\pi}{\sqrt{2}Wi} \quad (37)$$

in the limit $Pe \rightarrow \infty$, which is independent of pL . Hence, activity enhances shear thinning considerably.

Shear thinning of passive polymers, where $Pe = 0$, has intensively been studied experimentally [90,91], theoretically [88], and by simulations [89,92–97]. Specifically, measurements on DNA molecules provided insight into the behavior of individual polymers [91]. These experiments and simulations often predicted a power-law decay of the viscosity in the shear-thinning regime, with exponents in the range 1/2 to 2/3. The spread is partially explained by the very broad crossover regime between the zero-shear viscosity and the asymptotic dependence for $Wi \rightarrow \infty$. In any case, activity is predicted to lead to a significantly stronger shear-thinning effect.

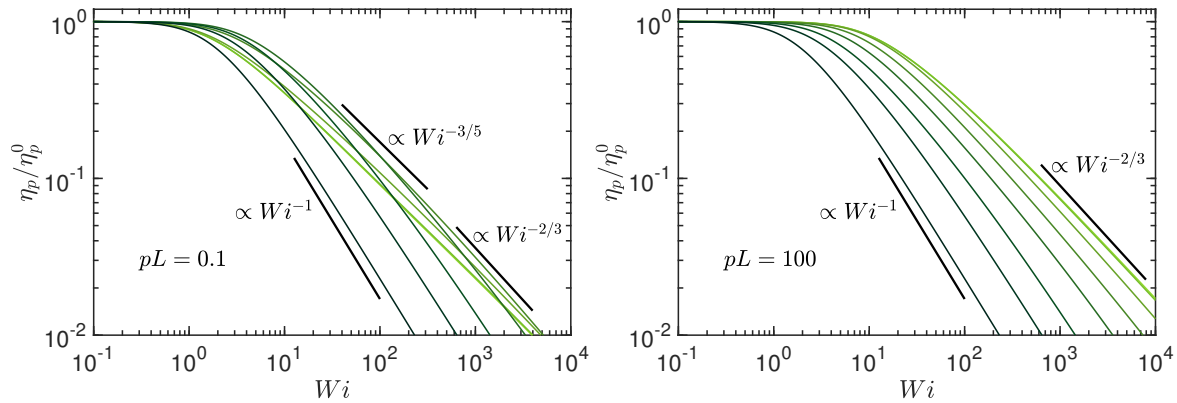


Figure 10. Shear viscosity η_p normalized by the viscosity η_p^0 of a non-sheared, active polymer as function of the Weissenberg number Wi for the Péclet numbers $Pe = 0, 0.6, 3, 10, 30, 10^2, 3 \times 10^2$, and ∞ (bright to dark color); (left) $pL = 0.1$ and (right) $pL = 10^2$. The number of active sites is $L/l = 10^2$ and $\Delta = 0.3$.

5. Discussion

The coupling between shear flow and activity, as is visible in the correlation functions (16)–(18), determines the characteristics of an ABPO in shear flow. The shear-rate dependence of all properties—conformational, dynamical, and rheological—are modified by activity. Thereby, the determining factor is the polymer inextensibility, which is reflected in the activity and shear-rate dependence of the stretching coefficient $\lambda = 3p\mu/2$ in our coarse-grained description. In particular, the asymptotic behavior for $Pe, Wi \rightarrow \infty$ is naturally governed by inextensibility. As far as the dynamics is concerned, we find a weaker variation of the relaxation times with shear rate at large activities compared to a passive polymer, with the longest relaxation time τ_1 changing from a $\tau_1 \sim Wi^{-2/3}$ dependence of a passive polymer to a $\tau_1 \sim Wi^{-1/2}$ decay for $Pe \gg 1$. In turn, this results in a change of the shrinkage of the radius of gyration components $G_{yy} = G_{zz}$ from a $Wi^{-2/3}$ to a Wi^{-1} dependence, a similar change for the viscosity η_p , and a change of the alignment from a $Wi^{-1/3}$ to a $Wi^{-1/2}$ dependence with increasing Wi at $Pe \gg 1$. As has already been discussed in Ref. [52], flexible and semiflexible ABPO show the same activity-induced swelling behavior for $Pe \gg 1$, independent of pL . Consequently, a universal shear-flow behavior is obtained in that limit. For all conformational (G_{xx} , G_{yy} , $\tan(2\chi_G)$), dynamical (τ_1), and rheological (η_p) properties, universal curves are obtained, with shear-rate dependencies differing from those of a passive system. The behavior originates from the dominance of the flexible modes (n^2) in the relaxation behavior for all stiffness caused by activity.

Active dumbbells already exhibit various of the discussed shear-induced characteristics [51]. However, the polymer nature, with the many more internal degrees of freedom, provides additional features and means of controlling active properties. Specifically, the number of active sites, L/l , is important. As our study shows, the crossover from the power laws valid for passive polymers to those of an ABPO at $P \gg 1$ depends crucially on L/l . With increasing L/l , the power laws for $Pe \gg 1$ appear at much larger Weissenberg numbers only. Depending on the size of the polymer, the Weissenberg numbers of the crossover could exceed experimentally accessible values. For computer simulations of an ABPO described as bead-spring polymer [57,86], this aspect is of minor concern because typically every monomer is considered as an ABP and not too long polymers are studied.

6. Conclusions

We have presented analytical results for active semiflexible polymers under shear flow. The Gaussian semiflexible polymer model is adopted, which takes into account the polymer inextensibility in a mean-field manner by a constraint for the contour length [75,80,82]. Activity is modeled as a colored noise force with an exponential temporal correlation. The linearity of the equation of motion, even in the presence of shear flow, allows for its analytical solution.

We have calculated the relaxation times, deformation, alignment, and viscosity as a function of shear rate. Each of these quantities shows a strong dependence on shear rate. Thereby, activity affects the shear response. An important aspect of a polymer in shear flow is its stretching and alignment along the flow direction, and its shrinkage transverse to it [88,89,95]. Activity enhances these aspects for flexible polymers. Semiflexible polymers show a nonmonotonic deformation behavior as a result of an activity-induced shrinkage at moderate Péclet numbers and a swelling at larger Pe , where the latter is similar to that of flexible polymers at the same Pe [52]. The activity-induced preference in alignment leads to a more pronounced shear thinning of highly active polymers, i.e., activity enhances shear thinning. All polymers exhibit the same shear-rate dependence in the limit $Pe \rightarrow \infty$, and, consequently, a universal behavior is obtained.

The active polymer relaxation behavior is governed by two processes, namely the diffusive dynamics of the active velocity, characterized by γ_R , and the relaxation times of the polymer. It remains to be analyzed how these competing processes determine the overall relaxation dynamics, e.g., of the end-to-end vector, and diffusion of the ABPO in the presence of shear flow.

Author Contributions: R.G.W. and G.G. conceived and designed the theoretical study; A.M.-G. and R.G.W. performed the analytical calculations; R.G.W., A.M.-G., and G.G. wrote the paper.

Funding: This research was funded by the European Union's Horizon 2020 research and innovation programme under Grant agreement No. 674979-NANOTRANS, and by the Deutsche Forschungsgemeinschaft (DFG) within the priority program SPP 1726 "Microswimmers—from Single Particle Motion to Collective Behaviour".

Conflicts of Interest: The authors declare no conflict of interest. The founding sponsors had no role in the design of the study; in the collection, analyses, or interpretation of data; in the writing of the manuscript, and in the decision to publish the results.

References

1. Ramaswamy, S. The mechanics and statistics of active matter. *Annu. Rev. Condens. Matter Phys.* **2010**, *1*, 323–345. [[CrossRef](#)]
2. Romanczuk, P.; Bär, M.; Ebeling, W.; Lindner, B.; Schimansky-Geier, L. Active Brownian Particles. *Eur. Phys. J. Spec. Top.* **2012**, *202*, 1–162. [[CrossRef](#)]
3. Marchetti, M.C.; Joanny, J.F.; Ramaswamy, S.; Liverpool, T.B.; Prost, J.; Rao, M.; Simha, R.A. Hydrodynamics of soft active matter. *Rev. Mod. Phys.* **2013**, *85*, 1143. [[CrossRef](#)]
4. Elgeti, J.; Winkler, R.G.; Gompper, G. Physics of microswimmers—Single particle motion and collective behavior: A review. *Rep. Prog. Phys.* **2015**, *78*, 056601. [[CrossRef](#)] [[PubMed](#)]
5. Bechinger, C.; Di Leonardo, R.; Löwen, H.; Reichhardt, C.; Volpe, G.; Volpe, G. Active particles in complex and crowded environments. *Rev. Mod. Phys.* **2016**, *88*, 045006. [[CrossRef](#)]
6. Marchetti, M.C.; Fily, Y.; Henkes, S.; Patch, A.; Yllanes, D. Minimal model of active colloids highlights the role of mechanical interactions in controlling the emergent behavior of active matter. *Curr. Opin. Colloid Interface Sci.* **2016**, *21*, 34–43. [[CrossRef](#)]
7. Winkler, R.G.; Elgeti, J.; Gompper, G. Active Polymers—Emergent Conformational and Dynamical Properties: A Brief Review. *J. Phys. Soc. Jpn.* **2017**, *86*, 101014. [[CrossRef](#)]
8. Lauga, E.; Powers, T.R. The hydrodynamics of swimming microorganisms. *Rep. Prog. Phys.* **2009**, *72*, 096601. [[CrossRef](#)]
9. Vicsek, T.; Zafeiris, A. Collective motion. *Phys. Rep.* **2012**, *517*, 71–140. [[CrossRef](#)]
10. Wysocki, A.; Winkler, R.G.; Gompper, G. Cooperative motion of active Brownian spheres in three-dimensional dense suspensions. *EPL* **2014**, *105*, 48004. [[CrossRef](#)]
11. Zöttl, A.; Stark, H. Emergent behavior in active colloids. *J. Phys. Condens. Matter* **2016**, *28*, 253001. [[CrossRef](#)]
12. Duman, O.; Isele-Holder, R.E.; Elgeti, J.; Gompper, G. Collective dynamics of self-propelled semiflexible filaments. *Soft Matter* **2018**, *14*, 4483–4494. [[CrossRef](#)] [[PubMed](#)]
13. Martin-Gomez, A.; Levis, D.; Diaz-Guilera, A.; Pagonabarraga, I. Collective motion of active Brownian particles with polar alignment. *Soft Matter* **2018**, *14*, 2610–2618. [[CrossRef](#)] [[PubMed](#)]
14. Muddana, H.S.; Sengupta, S.; Mallouk, T.E.; Sen, A.; Butler, P.J. Substrate Catalysis Enhances Single-Enzyme Diffusion. *J. Am. Chem. Soc.* **2010**, *132*, 2110–2111. [[CrossRef](#)] [[PubMed](#)]

15. Dey, K.K.; Das, S.; Poyton, M.F.; Sengupta, S.; Butler, P.J.; Cremer, P.S.; Sen, A. Chemotactic Separation of Enzymes. *ACS Nano* **2014**, *8*, 11941–11949. [[CrossRef](#)] [[PubMed](#)]
16. Nédélec, F.J.; Surrey, T.; Maggs, A.C.; Leibler, S. Self-organization of microtubules and motors. *Nature* **1997**, *389*, 305. [[CrossRef](#)] [[PubMed](#)]
17. Howard, J. *Mechanics of Motor Proteins and the Cytoskeleton*; Sinauer Associates: Sunderland, MA, USA, 2001.
18. Kruse, K.; Joanny, J.F.; Jülicher, F.; Prost, J.; Sekimoto, K. Asters, Vortices, and Rotating Spirals in Active Gels of Polar Filaments. *Phys. Rev. Lett.* **2004**, *92*, 078101. [[CrossRef](#)] [[PubMed](#)]
19. Bausch, A.R.; Kroy, K. A bottom-up approach to cell mechanics. *Nat. Phys.* **2006**, *2*, 231. [[CrossRef](#)]
20. Jülicher, F.; Kruse, K.; Prost, J.; Joanny, J.F. Active behavior of the cytoskeleton. *Phys. Rep.* **2007**, *449*, 3–28. [[CrossRef](#)]
21. Schaller, V.; Weber, C.; Semmrich, C.; Frey, E.; Bausch, A.R. Polar patterns of driven filaments. *Nature* **2010**, *467*, 73. [[CrossRef](#)] [[PubMed](#)]
22. Prost, J.; Jülicher, F.; Joanny, J.F. Active gel physics. *Nat. Phys.* **2015**, *11*, 111. [[CrossRef](#)]
23. Berg, H.C. *E. Coli in Motion*; Biological and Medical Physics Series; Springer: New York, NY, USA, 2004.
24. Guasto, J.S.; Rusconi, R.; Stocker, R. Fluid Mechanics of Planktonic Microorganisms. *Ann. Rev. Fluid Mech.* **2011**, *44*, 373–400. [[CrossRef](#)]
25. Howse, J.R.; Jones, R.A.L.; Ryan, A.J.; Gough, T.; Vafabakhsh, R.; Golestanian, R. Self-Motile Colloidal Particles: From Directed Propulsion to Random Walk. *Phys. Rev. Lett.* **2007**, *99*, 048102. [[CrossRef](#)] [[PubMed](#)]
26. Volpe, G.; Buttinoni, I.; Vogt, D.; Kümmerer, H.J.; Bechinger, C. Microswimmers in patterned environments. *Soft Matter* **2011**, *7*, 8810–8815. [[CrossRef](#)]
27. Thutupalli, S.; Seemann, R.; Herminghaus, S. Swarming behavior of simple model squirmers. *New J. Phys.* **2011**, *13*, 073021. [[CrossRef](#)]
28. Hagen, B.; Kümmel, F.; Wittkowski, R.; Takagi, D.; Löwen, H.; Bechinger, C. Gravitaxis of asymmetric self-propelled colloidal particles. *Nat. Commun.* **2014**, *5*, 4829. [[CrossRef](#)] [[PubMed](#)]
29. Maass, C.C.; Krüger, C.; Herminghaus, S.; Bahr, C. Swimming Droplets. *Annu. Rev. Condens. Matter Phys.* **2016**, *7*, 171–193. [[CrossRef](#)]
30. Copeland, M.F.; Weibel, D.B. Bacterial swarming: A model system for studying dynamic self-assembly. *Soft Matter* **2009**, *5*, 1174–1187. [[CrossRef](#)] [[PubMed](#)]
31. Selander, E.; Jakobsen, H.H.; Lombard, F.; Kiørboe, T. Grazer cues induce stealth behavior in marine dinoflagellates. *Proc. Natl. Acad. Sci. USA* **2011**, *108*, 4030–4034. [[CrossRef](#)] [[PubMed](#)]
32. Sohn, M.H.; Seo, K.W.; Choi, Y.S.; Lee, S.J.; Kang, Y.S.; Kang, Y.S. Determination of the swimming trajectory and speed of chain-forming dinoflagellate *Cochlodinium polykrikoides* with digital holographic particle tracking velocimetry. *Mar. Biol.* **2011**, *158*, 561–570. [[CrossRef](#)]
33. Yan, J.; Han, M.; Zhang, J.; Xu, C.; Luijten, E.; Granick, S. Reconfiguring active particles by electrostatic imbalance. *Nat. Mater.* **2016**, *15*, 1095. [[CrossRef](#)] [[PubMed](#)]
34. Löwen, H. Active colloidal molecules. *EPL* **2018**, *121*, 58001. [[CrossRef](#)]
35. Liverpool, T.B.; Maggs, A.C.; Ajdari, A. Viscoelasticity of Solutions of Motile Polymers. *Phys. Rev. Lett.* **2001**, *86*, 4171. [[CrossRef](#)] [[PubMed](#)]
36. Sarkar, D.; Thakur, S.; Tao, Y.G.; Kapral, R. Ring closure dynamics for a chemically active polymer. *Soft Matter* **2014**, *10*, 9577–9584. [[CrossRef](#)] [[PubMed](#)]
37. Chelakkot, R.; Gopinath, A.; Mahadevan, L.; Hagan, M.F. Flagellar dynamics of a connected chain of active, polar, Brownian particles. *J. R. Soc. Interface* **2014**, *11*, 20130884. [[CrossRef](#)] [[PubMed](#)]
38. Loi, D.; Mossa, S.; Cugliandolo, L.F. Non-conservative forces and effective temperatures in active polymers. *Soft Matter* **2011**, *7*, 10193–10209. [[CrossRef](#)]
39. Harder, J.; Valeriani, C.; Cacciuto, A. Activity-induced collapse and reexpansion of rigid polymers. *Phys. Rev. E* **2014**, *90*, 062312. [[CrossRef](#)] [[PubMed](#)]
40. Ghosh, A.; Gov, N.S. Dynamics of Active Semiflexible Polymers. *Biophys. J.* **2014**, *107*, 1065–1073. [[CrossRef](#)] [[PubMed](#)]
41. Shin, J.; Cherstvy, A.G.; Kim, W.K.; Metzler, R. Facilitation of polymer looping and giant polymer diffusivity in crowded solutions of active particles. *New J. Phys.* **2015**, *17*, 113008. [[CrossRef](#)]
42. Isele-Holder, R.E.; Elgeti, J.; Gompper, G. Self-propelled worm-like filaments: Spontaneous spiral formation, structure, and dynamics. *Soft Matter* **2015**, *11*, 7181–7190. [[CrossRef](#)] [[PubMed](#)]

43. Isele-Holder, R.E.; Jager, J.; Saggiorato, G.; Elgeti, J.; Gompper, G. Dynamics of self-propelled filaments pushing a load. *Soft Matter* **2016**, *12*, 8495–8505. [[CrossRef](#)] [[PubMed](#)]
44. Laskar, A.; Adhikari, R. Brownian microhydrodynamics of active filaments. *Soft Matter* **2015**, *11*, 9073–9085. [[CrossRef](#)] [[PubMed](#)]
45. Jiang, H.; Hou, Z. Motion transition of active filaments: Rotation without hydrodynamic interactions. *Soft Matter* **2014**, *10*, 1012–1017. [[CrossRef](#)] [[PubMed](#)]
46. Babel, S.; Löwen, H.; Menzel, A.M. Dynamics of a linear magnetic “microswimmer molecule”. *EPL* **2016**, *113*, 58003. [[CrossRef](#)]
47. Kaiser, A.; Löwen, H. Unusual swelling of a polymer in a bacterial bath. *J. Chem. Phys.* **2014**, *141*, 044903. [[CrossRef](#)] [[PubMed](#)]
48. Valeriani, C.; Li, M.; Novosel, J.; Arlt, J.; Marenduzzo, D. Colloids in a bacterial bath: Simulations and experiments. *Soft Matter* **2011**, *7*, 5228–5238. [[CrossRef](#)]
49. Suma, A.; Gonnella, G.; Marenduzzo, D.; Orlandini, E. Motility-induced phase separation in an active dumbbell fluid. *EPL* **2014**, *108*, 56004. [[CrossRef](#)]
50. Cugliandolo, L.F.; Gonnella, G.; Suma, A. Rotational and translational diffusion in an interacting active dumbbell system. *Phys. Rev. E* **2015**, *91*, 062124. [[CrossRef](#)] [[PubMed](#)]
51. Winkler, R.G. Dynamics of flexible active Brownian dumbbells in the absence and the presence of shear flow. *Soft Matter* **2016**, *12*, 3737–3749. [[CrossRef](#)] [[PubMed](#)]
52. Eisenstecken, T.; Gompper, G.; Winkler, R.G. Conformational Properties of Active Semiflexible Polymers. *Polymers* **2016**, *8*, 304. [[CrossRef](#)]
53. Eisenstecken, T.; Gompper, G.; Winkler, R.G. Internal dynamics of semiflexible polymers with active noise. *J. Chem. Phys.* **2017**, *146*, 154903. [[CrossRef](#)] [[PubMed](#)]
54. Siebert, J.T.; Letz, J.; Speck, T.; Virnau, P. Phase behavior of active Brownian disks, spheres, and dimers. *Soft Matter* **2017**, *13*, 1020–1026. [[CrossRef](#)] [[PubMed](#)]
55. Küchler, N.; Löwen, H.; Menzel, A.M. Getting drowned in a swirl: Deformable bead-spring model microswimmers in external flow fields. *Phys. Rev. E* **2016**, *93*, 022610. [[CrossRef](#)] [[PubMed](#)]
56. Kokot, G.; Das, S.; Winkler, R.G.; Gompper, G.; Aranson, I.S.; Snezhko, A. Active turbulence in a gas of self-assembled spinners. *Proc. Natl. Acad. Sci. USA* **2017**, *114*, 12870–12875. [[CrossRef](#)] [[PubMed](#)]
57. Eisenstecken, T.; Ghavami, A.; Mair, A.; Gompper, G.; Winkler, R.G. Conformational and dynamical properties of semiflexible polymers in the presence of active noise. *AIP Conf. Proc.* **2017**, *1871*, 050001.
58. Laskar, A.; Singh, R.; Ghose, S.; Jayaraman, G.; Kumar, P.B.S.; Adhikari, R. Hydrodynamic instabilities provide a generic route to spontaneous biomimetic oscillations in chemomechanically active filaments. *Sci. Rep.* **2013**, *3*, 1964. [[CrossRef](#)] [[PubMed](#)]
59. Vandebroek, H.; Vanderzande, C. Dynamics of a polymer in an active and viscoelastic bath. *Phys. Rev. E* **2015**, *92*, 060601. [[CrossRef](#)] [[PubMed](#)]
60. Sanchez, T.; Chen, D.T.N.; DeCamp, S.J.; Heymann, M.; Dogic, Z. Spontaneous motion in hierarchically assembled active matter. *Nature* **2012**, *491*, 431. [[CrossRef](#)] [[PubMed](#)]
61. Schaller, V.; Weber, C.; Frey, E.; Bausch, A.R. Polar pattern formation: Hydrodynamic coupling of driven filaments. *Soft Matter* **2011**, *7*, 3213–3218. [[CrossRef](#)]
62. Abkenar, M.; Marx, K.; Auth, T.; Gompper, G. Collective behavior of penetrable self-propelled rods in two dimensions. *Phys. Rev. E* **2013**, *88*, 062314. [[CrossRef](#)] [[PubMed](#)]
63. Denk, J.; Huber, L.; Reithmann, E.; Frey, E. Active Curved Polymers Form Vortex Patterns on Membranes. *Phys. Rev. Lett.* **2016**, *116*, 178301. [[CrossRef](#)] [[PubMed](#)]
64. Peruani, F. Active Brownian rods. *Eur. Phys. J. Spec. Top.* **2016**, *225*, 2301–2317. [[CrossRef](#)]
65. Needleman, D.; Dogic, Z. Active matter at the interface between materials science and cell biology. *Nat. Rev. Mater.* **2017**, *2*, 201748. [[CrossRef](#)]
66. Prathyusha, K.R.; Henkes, S.; Sknepnek, R. Dynamically generated patterns in dense suspensions of active filaments. *Phys. Rev. E* **2018**, *97*, 022606. [[CrossRef](#)] [[PubMed](#)]
67. Brangwynne, C.P.; Koenderink, G.H.; MacKintosh, F.C.; Weitz, D.A. Nonequilibrium Microtubule Fluctuations in a Model Cytoskeleton. *Phys. Rev. Lett.* **2008**, *100*, 118104. [[CrossRef](#)] [[PubMed](#)]
68. Weber, C.A.; Suzuki, R.; Schaller, V.; Aranson, I.S.; Bausch, A.R.; Frey, E. Random bursts determine dynamics of active filaments. *Proc. Natl. Acad. Sci. USA* **2015**, *112*, 10703–10707. [[CrossRef](#)] [[PubMed](#)]

69. Weber, S.C.; Spakowitz, A.J.; Theriot, J.A. Nonthermal ATP-dependent fluctuations contribute to the in vivo motion of chromosomal loci. *Proc. Natl. Acad. Sci. USA* **2012**, *109*, 7338–7343. [[CrossRef](#)] [[PubMed](#)]
70. Javer, A.; Long, Z.; Nugent, E.; Grisi, M.; Siriawatwetchakul, K.; Dorfman, K.D.; Cicuta, P.; Cosentino Lagomarsino, M. Short-time movement of *E. coli* chromosomal loci depends on coordinate and subcellular localization. *Nat. Commun.* **2013**, *4*, 3003. [[CrossRef](#)] [[PubMed](#)]
71. Zidovska, A.; Weitz, D.A.; Mitchison, T.J. Micron-scale coherence in interphase chromatin dynamics. *Proc. Natl. Acad. Sci. USA* **2013**, *110*, 15555. [[CrossRef](#)] [[PubMed](#)]
72. Winkler, R.G.; Wysocki, A.; Gompper, G. Virial pressure in systems of spherical active Brownian particles. *Soft Matter* **2015**, *11*, 6680–6691. [[CrossRef](#)] [[PubMed](#)]
73. Das, S.; Gompper, G.; Winkler, R.G. Confined active Brownian particles: Theoretical description of propulsion-induced accumulation. *New J. Phys.* **2018**, *20*, 015001. [[CrossRef](#)]
74. Barry, M.T.; Rusconi, R.; Guasto, J.S.; Stocker, R. Shear-induced orientational dynamics and spatial heterogeneity in suspensions of motile phytoplankton. *J. R. Soc. Interface* **2015**, *12*, 20150791. [[CrossRef](#)] [[PubMed](#)]
75. Winkler, R.G.; Reineker, P.; Harnau, L. Models and equilibrium properties of stiff molecular chains. *J. Chem. Phys.* **1994**, *101*, 8119–8129. [[CrossRef](#)]
76. Harnau, L.; Winkler, R.G.; Reineker, P. Dynamic properties of molecular chains with variable stiffness. *J. Chem. Phys.* **1995**, *102*, 7750–7757. [[CrossRef](#)]
77. Harnau, L.; Winkler, R.G.; Reineker, P. Dynamic Structure Factor of Semiflexible Macromolecules in Dilute Solution. *J. Chem. Phys.* **1996**, *104*, 6355–6368. [[CrossRef](#)]
78. Bawendi, M.G.; Freed, K.F. A Wiener integral model for stiff polymer chains. *J. Chem. Phys.* **1985**, *83*, 2491–2496. [[CrossRef](#)]
79. Battacharjee, S.M.; Muthukumar, M. Statistical mechanics of solutions of semiflexible chains: A path integral formulation. *J. Chem. Phys.* **1987**, *86*, 411–418. [[CrossRef](#)]
80. Ha, B.Y.; Thirumalai, D. A mean-field model for semiflexible chains. *J. Chem. Phys.* **1995**, *103*, 9408–9412. [[CrossRef](#)]
81. Winkler, R.G.; Reineker, P. Finite Size Distribution and Partition Functions of Gaussian Chains: Maximum Entropy Approach. *Macromolecules* **1992**, *25*, 6891–6896. [[CrossRef](#)]
82. Winkler, R.G. Deformation of Semiflexible Chains. *J. Chem. Phys.* **2003**, *118*, 2919–2928. [[CrossRef](#)]
83. Fodor, É.; Nardini, C.; Cates, M.E.; Tailleur, J.; Visco, P.; van Wijland, F. How Far from Equilibrium Is Active Matter? *Phys. Rev. Lett.* **2016**, *117*, 038103. [[CrossRef](#)] [[PubMed](#)]
84. Fily, Y.; Marchetti, M.C. Athermal Phase Separation of Self-Propelled Particles with No Alignment. *Phys. Rev. Lett.* **2012**, *108*, 235702. [[CrossRef](#)] [[PubMed](#)]
85. Bialké, J.; Speck, T.; Löwen, H. Crystallization in a Dense Suspension of Self-Propelled Particles. *Phys. Rev. Lett.* **2012**, *108*, 168301. [[CrossRef](#)] [[PubMed](#)]
86. Kaiser, A.; Babel, S.; ten Hagen, B.; von Ferber, C.; Löwen, H. How does a flexible chain of active particles swell? *J. Chem. Phys.* **2015**, *142*, 124905. [[CrossRef](#)] [[PubMed](#)]
87. Doi, M.; Edwards, S.F. *The Theory of Polymer Dynamics*; Clarendon Press: Oxford, UK, 1986.
88. Winkler, R.G. Conformational and rheological properties of semiflexible polymers in shear flow. *J. Chem. Phys.* **2010**, *133*, 164905. [[CrossRef](#)] [[PubMed](#)]
89. Huang, C.C.; Winkler, R.G.; Sutmann, G.; Gompper, G. Semidilute polymer solutions at equilibrium and under shear flow. *Macromolecules* **2010**, *43*, 10107. [[CrossRef](#)]
90. Bird, R.B.; Armstrong, R.C.; Hassager, O. *Dynamics of Polymer Liquids*; John Wiley & Sons: New York, NY, USA, 1987; Volume 1.
91. Schroeder, C.M.; Teixeira, R.E.; Shaqfeh, E.S.G.; Chu, S. Dynamics of DNA in the flow-gradient plane of steady shear flow: Observations and simulations. *Macromolecules* **2005**, *38*, 1967–1978. [[CrossRef](#)]
92. Lyulin, A.V.; Adolf, D.B.; Davies, G.R. Brownian dynamics simulations of linear polymers under shear flow. *J. Chem. Phys.* **1999**, *111*, 758–771. [[CrossRef](#)]
93. Jendrejack, R.M.; de Pablo, J.J.; Graham, M.D. Stochastic simulations of DNA in flow: Dynamics and the effects of hydrodynamic interactions. *J. Chem. Phys.* **2002**, *116*, 7752–7759. [[CrossRef](#)]
94. Liu, S.; Ashok, B.; Muthukumar, M. Brownian dynamics simulations of bead-rod-chain in simple shear flow and elongational flow. *Polymer* **2004**, *45*, 1383–1389. [[CrossRef](#)]

95. Aust, C.; Kröger, M.; Hess, S. Structure and dynamics of dilute polymer solutions under shear flow via nonequilibrium molecular dynamics. *Macromolecules* **1999**, *32*, 5660–5672. [[CrossRef](#)]
96. Eslami, H.; Müller-Plathe, F. Viscosity of Nanoconfined Polyamide-6,6 Oligomers: Atomistic Reverse Nonequilibrium Molecular Dynamics Simulation. *J. Phys. Chem. B* **2010**, *114*, 387–395. [[CrossRef](#)] [[PubMed](#)]
97. Singh, S.P.; Chatterji, A.; Gompper, G.; Winkler, R.G. Dynamical and rheological properties of ultrasoft colloids under shear flow. *Macromolecules* **2013**, *46*, 8026–8036. [[CrossRef](#)]



© 2018 by the authors. Licensee MDPI, Basel, Switzerland. This article is an open access article distributed under the terms and conditions of the Creative Commons Attribution (CC BY) license (<http://creativecommons.org/licenses/by/4.0/>).